International Journal of Mathematical Applications and Solutions
Vol 2, Issue 1 2026

Analytical soliton solutions of the (1+1)-dimensional Mikhailov-Novikov-Wang problem applied to the unified method: dynamical properties

Nithin Kumar[1], Sachin Kumar[2] †

Department of Mathematics,

Mathlogix publications

Article Info

Received: 18-12-2025 **Revised:24-01-2026** **Accepted:04-02-2026** **Published:15-02-2026**

Abstract

The (1+1)-dimensional Mikhailov-Novikov-Wang (MNW) equation is studied dynamically using the unified technique in this contribution. Solitons of various forms, such as those for trigonometric, periodic, exponential, elliptic, and other functions, are obtained using this method. Through the use of an efficient unified technique, this work's findings improve our comprehension of the equation's physical meaning and behaviour, illuminating the importance of studying various nonlinear wave phenomena in ocean engineering and physics. None of the other writers have ever used these derived findings in any of their prior studies. We use Mathematica to create 3-dimensional, contour, and 2-dimensional plots that show the answers in graphical form for the sake of presentation and physical examples. As a result, we find that several forms of soliton solutions, periodic solutions, anti-bell-shape solutions, kink wave solutions, solitary wave solutions, and multisoliton solutions are gained for the MNW equations.

Keywords: Analytical soliton solutions, unified method, solitons, Mikhailov-Novikov-Wang equation, dynamic nature, mathematical methods.

1 Introduction

Because of their widespread practical use, these nonlinear evolution equations have piqued the interest of many in the mathematical and physical sciences. Several complicated scientific events are usually explained by these equations. Optical fibres, fluid mechanics, plasma physics, and other fields have all made note of nonlinear evolution equations. The precise one-wave solutions to these complicated phenomena in fields as diverse as chemistry, plasma physics, nonlinear optics, biology, fluid dynamics, etc. have long been a goal of many mathematicians. Several powerful and efficient methods have been used by researchers to construct exact analytical solutions for these partial differential equations. These methods include the following: the Hirota method [1], the F-expansion method [2], the tanh function method [3], the modified extended Tanh expansion method [4, 5], the generalised Kudryashov method [6], the Darboux transformation method [7,8], the sine-cosine method [9], the Bäcklund transformation method [10,11], the Lie symmetry method [12–17], the Homogeneous balance method [18], the generalised exponential ratio-nal function method [19, 20], the generalised Riccati equation mapping (GREM) method [21,22], the unified method [23, 24], and many more [25–27]. If you need precise analytical answers, the unified approach is your best bet. Recent years have seen a proliferation of soliton solution types built by researchers using the unified method.

As a result, many nonlinear physics scientific phenomena may be better understood using MNW equation analysis [28, 29]. Not long ago, a number of scholars looked at the (1+1)-dimensional MNW equation. New soliton solutions were obtained by using the generalised projective Riccati equations approach, the singular manifold method, and the exp($\varphi(\xi)$)-expansion method to the problem by Raza et al. [30]. The kink-type multisoliton solutions of the MNW problem were found by Ray and Singh using the simplified Hirota's approach [31]. An precise solution was found by Akbulut et al. [32] using the generalised Kudryashov technique, the exponential rational function approach, and the modified extended tanh-function method. In their study, Bekir et al. [33] used the (G'/G)-expansion approach to find new accurate soliton solutions to the MNW problem, whereas we used a strong and effective unified strategy to build new analytical soliton solutions. Analysing this equation may provide

light on a plethora of fascinating nonlinear oceanographic and physical phenomena.

We provide a unified approach to solving the MNW problem analytically, with the goal of finding its precise solution. The following is an expression of the MNW equation [34–37] that we are considering:

$$u_{tt} - u_{xxxt} - 8u_x u_{xt} - 4u_t u_{xx} + 2u_x u_{xxxx} + 24u_x^2 u_{xx} + 4u_{xx} u_{xxx} = 0, \quad (1)$$

where $u = u(x,t)$ represents the wave amplitude. This equation derived by utilizing the perturbative symmetry method to the classification of integrable equations. Furthermore, MNW equation belongs to a hierarchy where the Boussinesq equation is a member of this class.

The used method is efficient, straightforward, and very powerful in order to investigate nonlinear partial differential equations (NPDEs) as they give a broad range of solitary wave solutions. Some families of exact analytical solutions of the MNW equation are studied via the help of *Wolfram Mathematica* for soft symbolic computation. By using this integral method, we derived analytical soliton solutions in the different form of solitary wave solutions, trigonometric solutions, hyperbolic solutions, soliton solutions, rational solutions, and many more kinds of solutions. All the obtained soliton solutions including few arbitrary constants and unknown coefficient parameters from the unified method have immense wide applications in mathematical science engineering. These obtained solutions are more beneficial and important in the area of fluid dynamics, optical physics, mathematical physics, plasma physics, and various fields of sciences. The newly exact analytical outcomes are illustrated in the diverse forms of anti-bell-shape solitons, kink waves, and periodic solitons. These obtained results are entirely new and never proposed in previous works done by other authors. Additionally, the wide range of dynamics, characteristics, and suitable arbitrary constant parameters of these new exact analytical results are depicted using 3-dimensional plots, contour plots, and 2-dimensional plots representation, with the appropriate selection of the employed rational functions, hyperbolic functions, trigonometric functions, and other arbitrary parameters. This kind of study shows positive results in the areas of development and advanced research.

We have organized this paper in the following sections: In section 2, we use a wave transformation to transform the MNW equation into an ordinary differential equation. In section 3, a detailed description of the proposed techniques is presented. Moreover, this section is devoted to the applications of the proposed methodology to (1+1)-dimensional Mikhailov-Novikov-Wang equation. In section 4, the results and discussion of the obtained solutions of the governing model are presented. Section 5 contains conclusions and important remarks.

2 Methodology of the unified method

Suppose that a general PDE is as follows,

$$\Phi(u_x,\ u_t,\ u_{xt},\ u_{xx}, u_{xxx}, \cdots) = 0. \tag{2}$$

Using the wave transformation

$$u(x,t) = U(\chi),\quad \chi = \zeta\ x - \delta\ t, \tag{3}$$

equation (2) converts into an ODE

$$\Theta(U',\ U'',\ U''\cdots) = 0, \tag{4}$$

in which ζ and δ real/complex constant parameters. The solution of equation (4) can furnish as follows

$$U(X) = G_0 + \sum_{i=1}^{N} G_i\ \xi(X)^i + \sum_{i=1}^{N} \frac{H_i}{\xi(X)^i}, \tag{5}$$

where $G_0,\ G_i,\ H_i\ (1 \le i \le N)$ are the unknown arbitrary parameters and explicit invariant solution $\xi(X)$ satisfies the following equation

$$\xi'(X) = \xi^2(X) + M. \tag{6}$$

In the three cases, equation (6) confirms nine types of exact solutions as follows.

Case 1: Hyperbolic function solutions (when M is negative)

$$\begin{aligned}
&(i)\quad \xi(X) = \frac{-\sqrt{-(P^2+Q^2)M} - P\sqrt{-M}\cosh(2\sqrt{-M}(X+\varphi))}{P\sinh(2\sqrt{-M}(X+\varphi)) + Q},\\
&(ii)\quad \xi(X) = \frac{-\sqrt{-(P^2+Q^2)M} - P\sqrt{-M}\cosh(2\sqrt{-M}(X+\varphi))}{P\sinh(2\sqrt{-M}(X+\varphi)) + Q},\\
&(iii)\quad \xi(X) = -\sqrt{-M} + \frac{2P\sqrt{-M}}{P+\cosh(2\sqrt{-M}(X+\varphi)) - \sinh(2\sqrt{-M}(X+\varphi))},\\
&(iv)\quad \xi(X) = \sqrt{-M} + \frac{2P\sqrt{-M}}{P+\cosh(2\sqrt{-M}(X+\varphi)) - \sinh(2\sqrt{-M}(X+\varphi))}.
\end{aligned} \tag{7}$$

Case 2: Trigonometric function solutions (when M is positive)

$$\begin{aligned}
&(v)\quad \xi(X) = \frac{\sqrt{(P^2+Q^2)M} - P\sqrt{M}\cos(2\sqrt{M}(X+\varphi))}{P\sin(2\sqrt{M}(X+\varphi)) + Q},\\
&(vi)\quad \xi(X) = \frac{-(P^2+Q^2)M - P\sqrt{M}\cos(2\sqrt{M}(X+\varphi))}{P\sin(2\sqrt{M}(X+\varphi)) + Q},\\
&(vii)\quad \xi(X) = -i\sqrt{M} + \frac{2iP\sqrt{M}}{P+\cos(2\sqrt{M}(X+\varphi)) - i\sin(2\sqrt{M}(X+\varphi))},
\end{aligned} \tag{8}$$

Case 3: Rational function solutions (when $M = 0$)

$$(ix) \quad \xi(X) = -\frac{1}{X + \varphi}, \tag{9}$$

when $P \neq 0$, φ and Q are arbitrary parameters.

3 Exact analytical solution of the MNW equation

The main objective of this section is to construct the exact analytical solutions of the MNW equation. Incorporating (3) and (1) yields

$$U'(\delta^2 + 12\zeta^2 U'(\delta + 2\zeta^2 U') + 4\zeta^5 U''') + \zeta^3(\delta + 2\zeta^2 U')U'''' = 0. \tag{10}$$

Integrating equation (10) with respect to χ and taking the integration constant zero, we obtained

$$6\zeta^2\delta(U')^2 + 8\zeta^4(U')^3 + \zeta^5(U'')^2 + \zeta^3\delta U''' + U'(\delta^2 + 2\zeta^5 U'') = 0. \tag{11}$$

With the help of the principle of balancing for $U'U'''$ and U'^3, we contain $N = 1$. Inserting $N = 1$ in equation (5), we have

$$U(X) = G_0 + G_1\xi(X) + \frac{H_1}{\xi(X)}. \tag{12}$$

Combining equation (6), (12) and (11), we get the following three solution sets

$$G_0 = G_0,\ G_1 = -2\zeta,\ H_1 = 0,\ \delta = 4\zeta^3 M, \tag{13}$$

$$G_0 = G_0,\ G_1 = 0,\ H_1 = 2\zeta M,\ \delta = 4\zeta^3 M, \tag{14}$$

$$G_0 = G_0,\ G_1 = -2\zeta,\ H_1 = 2\zeta M,\ \delta = 16\zeta^3 M. \tag{15}$$

Using equation (3), equation (7)-(9), and equation (13), we obtain the subsequent exact analytical solutions of the MNW equation (1)

$$u_{11}(x,t) = G_0 - 2\zeta \left(\frac{-\sqrt{-(P^2+Q^2)M} - P\sqrt{-M}\cosh(2\sqrt{-M}(\zeta x - 4\zeta^3 M t + \varphi))}{P\sinh(2\sqrt{-M}(\zeta x - 4\zeta^3 M t + \varphi)) + Q} \right), \tag{16}$$

$$u_{12}(x,t) = G_0 - 2\zeta \left(\frac{\sqrt{-(P^2+Q^2)M} - P\sqrt{-M}\cosh(2\sqrt{-M}(\zeta x - 4\zeta^3 M t + \varphi))}{P\sinh(2\sqrt{-M}(\zeta x - 4\zeta^3 M t + \varphi)) + Q} \right). \tag{17}$$

We can see various simulations of the solutions of the equation (17) in Figure 1.

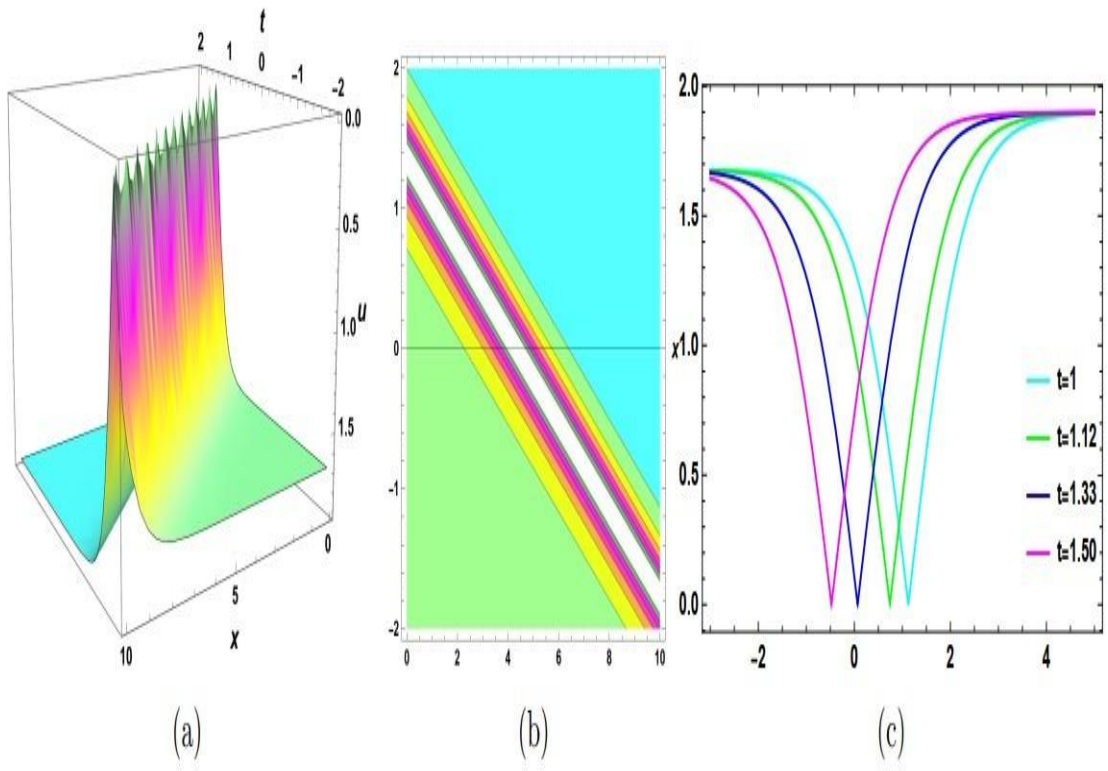


Fig. 1 Anti-bell-shape profile observed via 3D for the solutions of the equation (17) in this figure with the $G_0 = 0.11$, $\zeta = 2$, $P = 0.021$, $Q = 397$, $\varphi = 3$, $M = -0.2$ and wave propagation for different values of $t = 1,\ 1.12,\ 1.33,\ 1.50$ with the $-3 \leq x \leq 5$ shows through 2D plot.

$$u_{13}(x,t) = \frac{4\zeta P\sqrt{-M}}{\sinh(2\sqrt{-M}(\zeta x - 4\zeta^3 M t + \varphi)) - P - \cosh(2\sqrt{-M}(\zeta x - 4\zeta^3 M t + \varphi))} G_0 + 2\zeta\sqrt{-M},, \tag{18}$$

$$u_{14}(x,t) = \frac{4\zeta P\sqrt{-M}}{\sinh(2\sqrt{-M}(\zeta x - 4\zeta^3 M t + \varphi)) - P - \cosh(2\sqrt{-M}(\zeta x - 4\zeta^3 M t + \varphi))} + G_0 - 2\zeta\sqrt{-M}, \tag{19}$$

Various simulations of the solutions of the equation (19) may be observed by Figure 2.

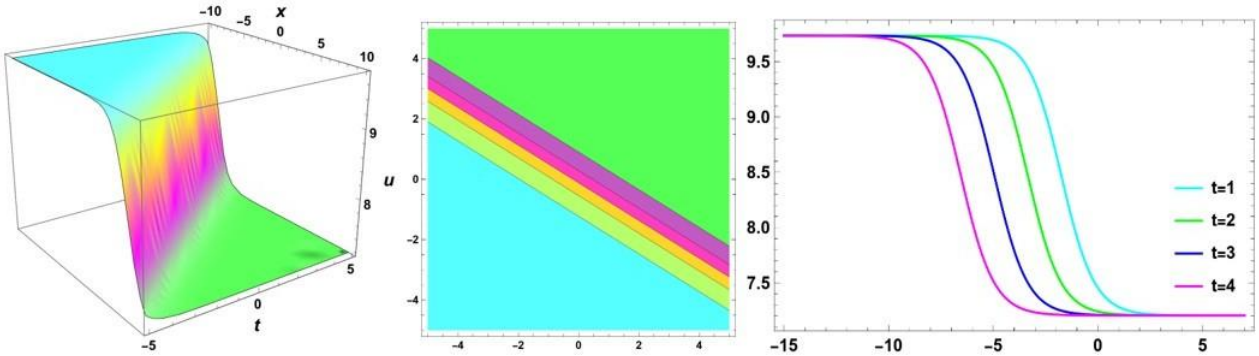


Fig. 2 Kink wave profile observed via 3D for the solutions of the equation (19) in this figures with the $G_0 = 11,\ \zeta = 2,\ P = 1,\ Q = 7,\ \varphi = 0.3,\ M = -0.1$ and wave propagation for different values of $t = 1,\ 2,\ 3,\ 4$ with the $-15 \le x \le 7$ shows through 2D Plot.

$$u_{15}(x,t) = G_0 + 2\zeta \frac{\sqrt{(P^2+Q^2)M} + P\sqrt{M}\cos(2\sqrt{M}(\zeta x - 4\zeta^3 M t + \varphi))}{P\sin(2\sqrt{M}(\zeta x - 4\zeta^3 M t + \varphi)) + Q}, \tag{20}$$

$$u_{16}(x,t) = G_0 - 2\zeta \frac{\sqrt{(P^2+Q^2)M} - P\sqrt{M}\cos(2\sqrt{M}(\zeta x - 4\zeta^3 M t + \varphi))}{P\sin(2\sqrt{M}(\zeta x - 4\zeta^3 M t + \varphi)) + Q},, \tag{21}$$

$$u_{17}(x,t) = -\frac{4i\zeta P\sqrt{M}}{P + \cos(2\sqrt{M}(\zeta x - 4\zeta^3 M t + \varphi)) - i\sin(2\sqrt{M}(\zeta x - 4\zeta^3 M t + \varphi))} G_0 + 2i\zeta\sqrt{M}, \tag{22}$$

$$u_{18}(x,t) = -\frac{4i\zeta P\sqrt{M}}{P + \cos(2\sqrt{M}(\zeta x - 4\zeta^3 M t + \varphi)) - i\sin(2\sqrt{M}(\zeta x - 4\zeta^3 M t + \varphi))} + G_0 - 2i\zeta\sqrt{M}, \tag{23}$$

$$u_{19}(x,t) = G_0 + \frac{2\zeta}{\zeta x - 4\zeta^3 M t + \varphi}. \tag{24}$$

Several views of the solutions of the equation (21) may be observed by Figure 3.

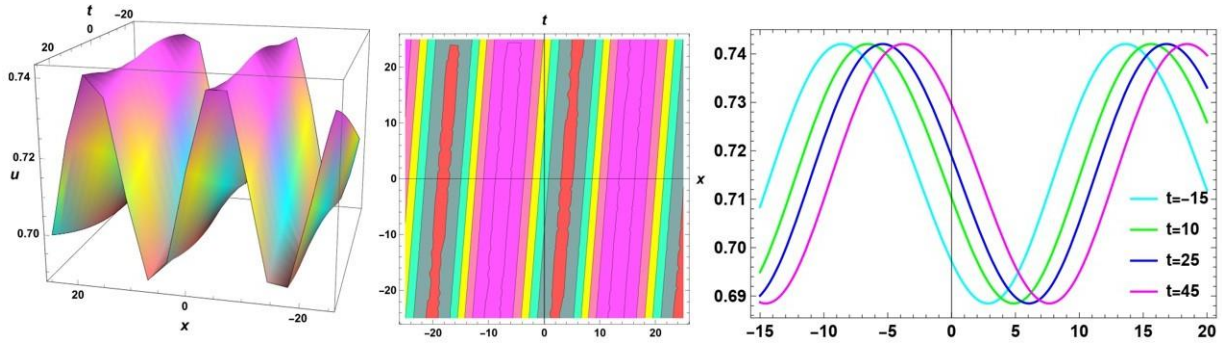


Fig. 3 Periodic wave profile observed via 3D for the solutions of the equation (21) in this figures with the $G_0 = 1,\ \zeta = 0.2,\ P = 0.2,\ Q = 3,\ \varphi = 2,\ M = 0.5$ and wave propagation for different values of $t = -15,\ 10,\ 25,\ 45$ with the $-15 \le x \le 20$ shows through 2D Plot.

Using equation (3), equation (7)-(9), and equation (14), we obtain the subsequent exact analytical solutions of the MNW equation (1)

$$u_{21}(x,t) = G_0 + 2\zeta M \left(\frac{P\sinh(2\sqrt{-M}(\zeta x - 4\zeta^3 M t + \varphi)) + Q}{-\sqrt{-(P^2+Q^2)M} - P\sqrt{-M}\cosh(2\sqrt{-M}(\zeta x - 4\zeta^3 M t + \varphi))} \right), \tag{25}$$

$$u_{22}(x,t) = G_0 + 2\zeta M \left(\frac{P\sinh(2\sqrt{-M}(\zeta x - 4\zeta^3 M t + \varphi)) + Q}{\sqrt{-(P^2+Q^2)M} - P\sqrt{-M}\cosh(2\sqrt{-M}(\zeta x - 4\zeta^3 M t + \varphi))} \right), \tag{26}$$

$$u_{23}(x,t) = G_0 + 2\zeta M \left(\sqrt{-M} - \frac{2P\sqrt{-M}}{P + \cosh(2\sqrt{-M}\Xi) - \sinh(2\sqrt{-M}\Xi)} \right)^{-1}, \tag{27}$$

$$u_{24}(x,t) = G_0 + 2\zeta M \left(\sqrt{-M} + \frac{2P\sqrt{-M}}{P + \cosh(2\sqrt{-M}\Xi) - \sinh(2\sqrt{-M}\Xi)} \right)^{-1}. \tag{28}$$

We may plot the several simulations of the solutions of the equation (26) in Figure 4.

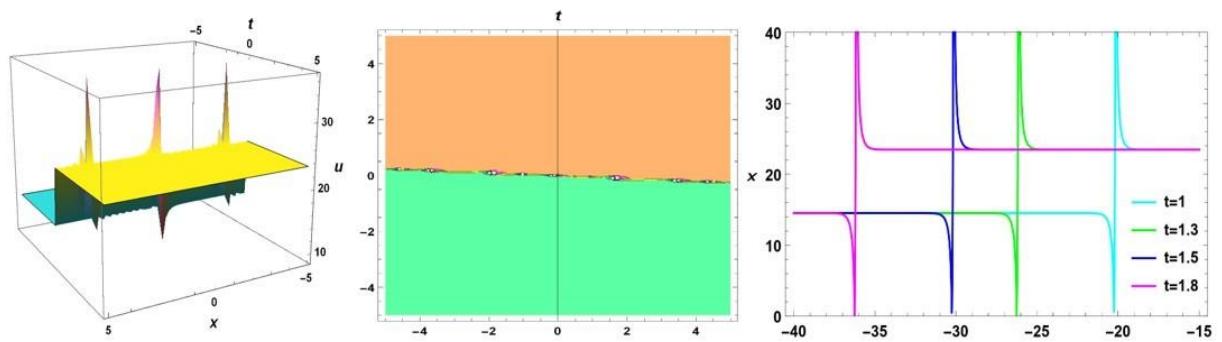


Fig. 4 Interaction between kink wave and soliton wave profile observed via 3D Plot for the solutions of the equation (26) in this figure with the $G_0 = 0.11,\ \zeta = 2,\ P = 0.021,\ Q = 397,\ \varphi = 3,\ M = -0.2$ and wave propagation for different values of $t = 1,\ 1.3,\ 1.5,\ 1.8$ with the $-5 \le x \le 5$ shows through 2D graph.

$$u_{25}(x,t) = G_0 + 2\zeta M \left(\frac{-\sqrt{(P^2+Q^2)M} - P\sqrt{M}\cos(2\sqrt{M}(\zeta x - 4\zeta^3 M t + \varphi))}{P\sin(2\sqrt{M}(\zeta x - 4\zeta^3 M t + \varphi)) + Q} \right), \tag{29}$$

$$u_{26}(x,t) = G_0 + 2\zeta M \left(\frac{P\sin(2\sqrt{M}(\zeta x - 4\zeta^3 M t + \varphi)) + Q}{\sqrt{(P^2+Q^2)M} - P\sqrt{M}\cos(2\sqrt{M}(\zeta x - 4\zeta^3 M t + \varphi))} \right), \tag{30}$$

$$u_{27}(x,t) = G_0 - 2\zeta M \left(i\sqrt{M} - \frac{2iP\sqrt{M}}{P + \cos(2\sqrt{M}\Xi) - i\sin(2\sqrt{M}\Xi)} \right)^{-1}, \tag{31}$$

$$u_{28}(x,t) = G_0 + 2\zeta M \left(i\sqrt{M} + \frac{2iP\sqrt{M}}{P + \cos(2\sqrt{M}\Xi) - i\sin(2\sqrt{M}\Xi)} \right)^{-1}, \tag{32}$$

$$u_{29}(x,t) = G_0 - 2\zeta M(\zeta x - 4\zeta^3 M t + \varphi), \tag{33}$$

where $\Xi = (\zeta x - 4\zeta^3 M t + \varphi)$. Figure 5 presents several simulations of the solutions of the equation (29).

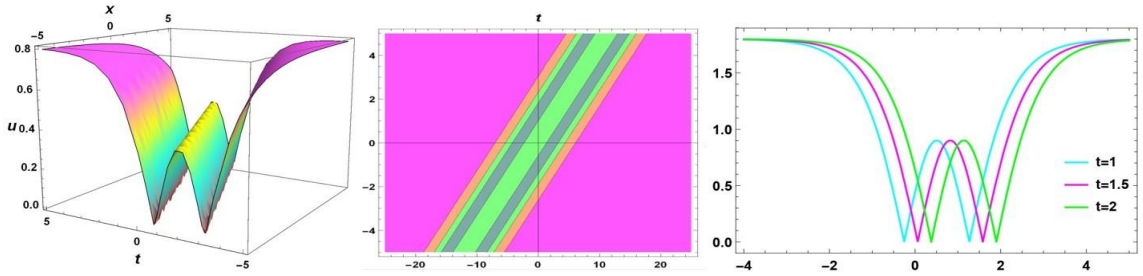


Fig. 5 W-shape wave profile observed via 3D for the solutions of the equation (29) in this figure with the $G_0 = 0.17$, $\zeta = 1.2$, $P = 0.61$, $Q = 1.7$, $\varphi = 3$, $M = 1$ and wave propagation for different values of $t = 1,\ 1.5,\ 2$ with the $-3 \le x \le 5$ shows through 2D plot.

Using equation (3), equation (7)-(9), and equation (15), we obtain the subsequent exact analytical solutions of the MNW equation (1)

$$u_{31}(x,t) = G_0 - 2\zeta \left(\frac{-\sqrt{-(P^2+Q^2)M} - P\sqrt{-M}\cosh(2\sqrt{-M}(\zeta x - 16\zeta^3 M t + \varphi))}{P\sinh(2\sqrt{-M}(\zeta x - 16\zeta^3 M t + \varphi)) + Q} \right)$$
$$+ 2\zeta M \left(\frac{P\sinh(2\sqrt{-M}(\zeta x - 16\zeta^3 M t + \varphi)) + Q}{\sqrt{-(P^2+Q^2)M} - P\sqrt{-M}\cosh(2\sqrt{-M}(\zeta x - 16\zeta^3 M t + \varphi))} \right), \tag{34}$$

$$u_{32}(x,t) = G_0 - 2\zeta \left(\frac{-\sqrt{-(P^2+Q^2)M} - P\sqrt{-M}\cosh(2\sqrt{-M}(\zeta x - 16\zeta^3 M t + \varphi))}{P\sinh(2\sqrt{-M}(\zeta x - 16\zeta^3 M t + \varphi)) + Q} \right)$$
$$+ 2\zeta M \left(\frac{P\sinh(2\sqrt{-M}(\zeta x - 16\zeta^3 M t + \varphi)) + Q}{\sqrt{-(P^2+Q^2)M} - P\sqrt{-M}\cosh(2\sqrt{-M}(\zeta x - 16\zeta^3 M t + \varphi))} \right). \tag{35}$$

Figure 6 introduces several simulations of the solutions of the equation (34).

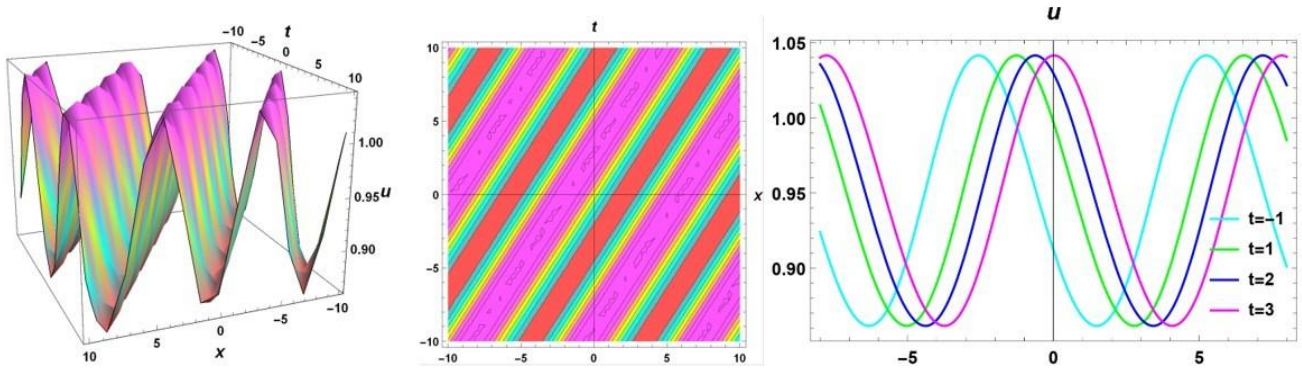


Fig. 6 Solitary wave profile observed via 3D for the solutions of the equation (34) in this figure with the $G_0 = 0.5,\ \zeta = 0.17,\ P = 3,\ Q = 6,\ \varphi = 23,\ M = -1.4$ and wave propagation for different values of $t = -1,\ 1,\ 2,\ 3$ with the $-10 \le x \le 10$ shows through 2D plot.

$$u_{33}(x,t) = \frac{4\zeta P\sqrt{-M}}{\sinh(2\sqrt{-M}(\zeta x - 16\zeta^3 M t + \varphi)) - P - \cosh(2\sqrt{-M}(\zeta x - 16\zeta^3 M t + \varphi))} G_0 + 2\zeta\sqrt{-M} + 2\zeta M\sqrt{-M} - \frac{2P\sqrt{-M}}{P + \cosh(2\sqrt{-M}\Xi_1) - \sinh(2\sqrt{-M}\Xi_1)}^{-1}, \quad (36)$$

$$u_{34}(x,t) = \frac{4\zeta P\sqrt{-M}}{\sinh(2\sqrt{-M}(\zeta x - 16\zeta^3 M t + \varphi)) - P - \cosh(2\sqrt{-M}(\zeta x - 16\zeta^3 M t + \varphi))} + G_0 - 2\zeta\sqrt{-M} + 2\zeta M\sqrt{-M} + \frac{2P\sqrt{-M}}{P + \cosh(2\sqrt{-M}\Xi_1) - \sinh(2\sqrt{-M}\Xi_1)}^{-1}, \quad (37)$$

$$u_{35}(x,t) = G_0 + 2\zeta \left(\frac{\sqrt{(P^2+Q^2)M} + P\sqrt{M}\cos(2\sqrt{M}(\zeta x - 16\zeta^3 M t + \varphi))}{P\sin(2\sqrt{M}(\zeta x - 16\zeta^3 M t + \varphi)) + Q}\right) + 2\zeta M \left(\frac{-\sqrt{(P^2+Q^2)M} - P\sqrt{M}\cos(2\sqrt{M}(\zeta x - 16\zeta^3 M t + \varphi))}{P\sin(2\sqrt{M}(\zeta x - 16\zeta^3 M t + \varphi)) + Q}\right), \quad (38)$$

$$u_{36}(x,t) = G_0 - 2\zeta \left(\frac{\sqrt{(P^2+Q^2)M} - P\sqrt{M}\cos(2\sqrt{M}(\zeta x - 16\zeta^3 M t + \varphi))}{P\sin(2\sqrt{M}(\zeta x - 16\zeta^3 M t + \varphi)) + Q}\right) + 2\zeta M \left(\frac{P\sin(2\sqrt{M}(\zeta x - 16\zeta^3 M t + \varphi)) + Q}{\sqrt{(P^2+Q^2)M} - P\sqrt{M}\cos(2\sqrt{M}(\zeta x - 16\zeta^3 M t + \varphi))}\right), \quad (39)$$

$$u_{37}(x,t) = -\frac{4i\zeta P\sqrt{M}}{P + \cos(2\sqrt{M}(\zeta x - 16\zeta^3 M t + \varphi)) - i\sin(2\sqrt{M}(\zeta x - 16\zeta^3 M t + \varphi))} G_0 + 2i\zeta\sqrt{M} - 2\zeta M\, i\sqrt{M} - \frac{2iP\sqrt{M}}{P + \cos(2\sqrt{M}\Xi_1) - i\sin(2\sqrt{M}\Xi_1)}^{-1}, \quad (40)$$

$$u_{38}(x,t) = -\frac{4i\zeta P\sqrt{M}}{P + \cos(2\sqrt{M}(\zeta x - 16\zeta^3 M t + \varphi)) - i\sin(2\sqrt{M}(\zeta x - 16\zeta^3 M t + \varphi))} + G_0 - 2i\zeta\sqrt{M} + 2\zeta M\, i\sqrt{M} + \frac{2iP\sqrt{M}}{P + \cos(2\sqrt{M}\Xi_1) - i\sin(2\sqrt{M}\Xi_1)}^{-1}, \quad (41)$$

$$u_{39}(x,t) = G_0 + \frac{2\,\zeta}{\zeta\, x - 16\zeta^3 M\, t + \varphi} - 2\,\zeta\, M(\zeta\, x - 16\zeta^3 M\, t + \varphi), \tag{42}$$

where $\Xi_1 = (\zeta\, x\, - 16\zeta^3 M\, t + \varphi)$. Via Figure 7, we observe the several simulations of the solutions of the equation (38).

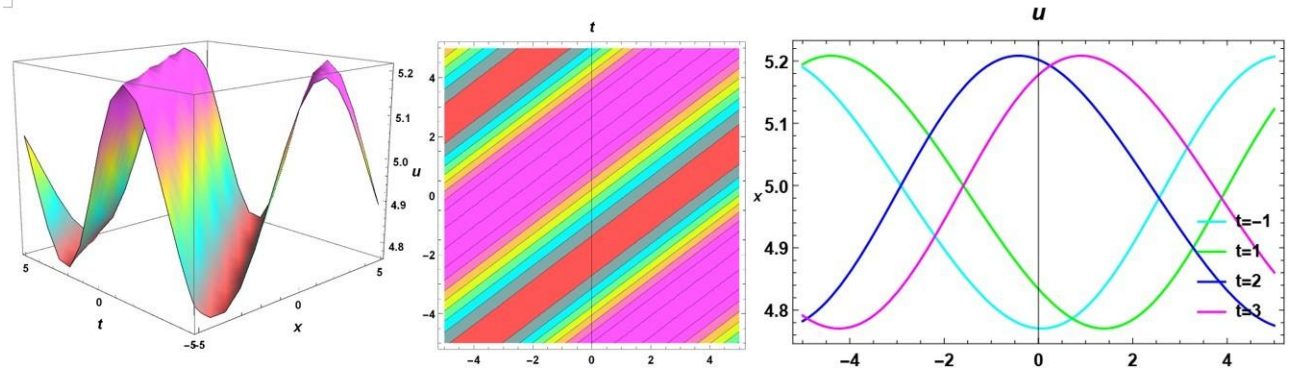


Fig. 7 Periodic wave profile observed via 3D for the solutions of the equation (38) in this figure with the $G_0 = 5, \zeta = 0.351, P = 0.4, Q = 3, \varphi = 13, M = 0.672$ and wave propagation for different values of $t = -1, 1, 2, 3$ with the $-5 \leq x \leq 5$ shows through 2D plot.

4 Result and discussion

Examining the analytic soliton solutions employing the powerful integral unified technique is new and different from the earlier results acquired by employing diverse approaches. We received the eclectic forms of analytical soliton wave solutions such as hyperbolic function, traveling wave, rational function, and trigonometric function solutions for the Mikhailov-Novikov-Wang equation. Consequently, our obtained solutions have been verified by using the symbolic computation *Mathematica* software after placing them back into the MNW equation. To explain the physical phenomena of these solutions via 3D, contour, and 2D plots by using the suitable values of unknown coefficients and arbitrary constant parameters, the observations are given in the following manner: Figures 1 and 2 show the anti-bell shape wave and kink shape wave profiles for solutions (17) and (19). Figures 3, 4, and 5 illustrate the evolutionary profile of solitary waves for solutions (21), (26), and (29). Figures 6 and 7 depict the interaction between soliton and kink wave and W-shape wave soliton profiles for solutions (34), and (38). The dynamical behavior of the analytical soliton solutions is presented by setting the suitable values of unknown coefficients and free parameter constants.

5 Conclusion

All things considered, we were able to get a wide variety of novel precise analytical solutions to the MNW problem under consideration by using the unified technique. Exact solutions of several types were obtained, including rational, trigonometric, exponential, hyperbolic, and combinations thereof with constant parameters of any sort. The approach that was used is superior to other analytical methods in terms of computing efficiency, power, and reliability. When compared to the findings found in the literature, the outcomes of the study are utterly different. To help clarify the action and character of the solutions, we included visual illustrations in our discussion. The 3D, contour, and 2D forms showcase the physical significance of the defined analytical solitary wave findings. As a

result, the solu-tions showed a variety of wave forms, including anti-bell-shape, kink wave, solitary wave, and periodic wave. totions (17), (19), (21), (26), (29), (34), and (38). Soliton wave structures provide a holistic perspective that shows how different physical and biological systems interact with one another. Research into a wide range of dynamical systems will benefit greatly from the expansion of fruitful analytical soliton findings. Plasma physics, mathematical physics, nonlinear waves, fluid dynamics, and nonlinear sciences may greatly benefit from the results produced using the technique presented in this study. Our study paves the way for several exciting new directions in the field of future research. The expansion of our methodology to address increasingly complex higher-order nonlinear evolution equations from areas including nonlinear sciences, mathematical physics, and plasma physics is one potential path.

References

[1] Cambridge University Press, 2004, 155. Hirota R., The Direct Method in Soliton Theory. Journal of Applied Mathematics, 2013(895760), 1-7, 2013. [2] Zhao Y.M., The F-expansion approach and its application for discovering novel precise solutions to the Kudryashov-Sinelshchikov problem. The tanh technique for travelling wave solutions of nonlinear equations was published in 2004 in Applied Mathematics and Computing, volume 154, issue 3, pages 713-723. [3] Wazwaz A.M. In 2008, Wazwaz published an article in Communications in Nonlinear Science and Numerical Simulation titled "The Extended Tanh Method for the Zakharov-Kuznestsov (ZK) equation, the modified ZK equation and its generalised forms," which went on to discuss other methods for solving this particular problem. In 2009, Ma and Lee published an article in Chaos, Solitons, and Fractals titled "A transformed rational function method and exact solutions to the (3+1) dimensional Jimbo-Miwa equation." The article spanned from pages 1356 to 1363.

In their 2021 article published in the Journal of Ocean Engineering and Science, Kumar S. and Kumar A. discuss the abundance of closed-form wave solutions and the dynamical structures of soliton solutions to the (3+1)-dimensional BLMP problem in mathematical physics. The paper spans pages 178 to 187. Cambridge University Press, Cambridge, UK, 2002, pp. 7–14. [7] Rogers, C., Schief, W.K., Bäcklund, and Darboux, Transformations: Geometry and Modern Applications in Soliton Theory. [8] In 1975, Wadati, Sanuki, and Konno published an article in the Progress of Theoretical Physics discussing the relations between the inverse technique, the Bäclaund transformation, and an infinite number of conservation laws. The article spanned from pages 419 to 436.

For the perturbed NLSE with Kerr law nonlinearity, Mahak and Akram (2019) extend rational sine-cosine and rational sinh-cosh approaches to extract solutions (134(159), 1–10). Ap-plied Mathematics Letters, Volume 25, Issue 10, Pages 1500–1504, 2012, by Ma W.X. and Abdeljabbar A., is a generalised KP equation in three dimensions plus one. Regarding the conformable nonlinear Schrödinger equation with second order spatiotemporal and group velocity dispersion coefficients, Rezazadeh et al. (2021) published in the Chinese Journal of Physics, page 403–414. [12] In their 2019 publication "Lie symmetry reductions and group invariant solutions of (2+1)-dimensional modified Veronese web equation," Kumar and Kumar discuss the topic in Nonlinear Dynamics, volume 98, pages 1891–1903. In 2020, Kumar S., Kumar A., and Kharbanda H. published an article in Physica Scripta titled "Lie symmetry analysis and generalised invariant solutions of (2+1)-dimensional dispersive long wave (DLW) equations" (95, 065207).

Closed-form invariant solutions from the Lie symmetry analysis and dynamics of the solitonic profiles for the (2+1)-dimensional modified Heisenberg ferromagnetic system were published in Modern Physics Letter B, volume 36, issue 7, pages 2150609, in 2022. The authors are Kumar A., Kumar S., and Kharbanda H. The authors Kumar and Kumar (2020) provide Lie symmetry analysis in their paper "Dynamic structures of solitons and some new types of exact solutions for the (2+1)-dimensional DJKM equation." The paper is published in Modern Physics Letters B and can be found on page 2150015.

In the Chinese Journal of Physics, Kumar et al. (2021) discuss Lie symmetries, optimum systems, and group-invariant solutions to the (3+1)-dimensional generalised KP equation. The paper is located on page 69 and runs from page 1 to 23.

The authors of the following work published in 2021 in Chaos Solitons and Fractals: Kumar A., Kumar D., and

Kumar S., Lie symmetry analysis for getting the plentiful precise solutions, optimum system, and dynamics of solitons for a higher-dimensional Fokas equation, 142, 110507.
Solitary wave solutions for variant Boussinesq equations were published in 1995 in Physics Letters A, volume 199, issues 3–4, pages 169–72.
In 2018, Ghanbari and Inc. published an article in The European Physical Journal Plus describing a novel approach to solving the resonance nonlinear Schrödinger equation using generalised exponential rational functions. The article can be found on pages 133–142.
In their 2020 publication titled "New exact solitary wave solutions of the strain wave equation in microstructured solids via the generalised exponential rational function method," Kumar S., Wazwaz A.M., and Kumar A. published in The European Physical Journal Plus, the authors provide new findings in the field.
In a Zig-Zag optical lattice model with two integral schemes, Kumar A. and Kumar S. (2022) study the dynamical behaviours and numerous optical soliton solutions of cold bosonic atoms. The results are published in Mathematics and Computers in Simulation, volume 201, pages 254-274.
(22), Kumar S. and Kumar A., Optical and Quantum Electronics, 55, 566, 2023, newly produced optical wave solutions and dynamical behaviours of the highly nonlinear coupled Davey-Stewartson Fokas system in monomode optical fibres.
"Unification of all hyperbolic tangent function methods" was published in 2016 in Open Physics by Gözükızıl Ö.F., Akçagɔıl S., and Aydemir T.
In 2018, a novel application of the unified technique was published in the novel Trends in Mathematical Sciences, volume 6, issue 1, pages 185 to 199, by Akçag˘ıl and Aydemir.
[25] In Optik, 287, 171060, 2023, Das and Ray provide exact travelling wave and soliton solutions to the conformable M-fractional modified nonlinear Schrödinger model.
Journal of Nonlinear Optical Physics and Materials, 2023, DOI:10.1142/S0218863523500753, Das N., Ray S.S., Highly dispersive optical solitons and solitary wave solutions for the (2+1)-dimensional Mel'nikov equation in modelling interaction of long waves with short wave packets in two dimensions.
Nonlinear Dynamics, 111, 16367-16376 (2023), by Wu J., presents a new universal nonlocal reverse-time nonlinear Schrödinger equation and the Riemann-Hilbert technique for solving it.
In 2007, Mikhailov, Novikov, and Wang published an article in Studies in Applied Mathematics titled "On classification of integrable nonevolutionary equations" (118(4), 419-457).
In their 2002 article "Perturbative symmetry approach," Mikhailov and Novikov discussed the topic in the Journal of Physics A: Mathematical and General, volume 35, issue 22, pages 4775.
In their 2022 article published in the Journal of Geometry and Physics, Raza, Seadawy, Arshed, and Rafiq discuss three analytical approaches that provide a range of soliton solutions to the Mikhailov-Novikov-Wang dynamical equation (176, 104515).